

Effect of kissing bond on fatigue behavior of friction stir welds on Al 5083 alloy

CAIZHI ZHOU, XINQI YANG*

School of Materials Science and Engineering, Tianjin University, Tianjin 300072, People's Republic of China

E-mail: xqyang@tju.edu.cn

GUOHONG LUAN

China FSW Center Beijing FSW Technology Limited Company, Beijing 100024, People's Republic of China

Published online: 9 March 2006

Fatigue properties of FS welds with a kissing bond (bonded welds) were studied by comparing the test results of bonded welds with those of sound welds. The fatigue life of bonded welds is 21 ~ 43 times shorter than that of sound welds under the stress ratio $R = 0.1$, and the fatigue characteristic values of each welds have decreased from 100.24 MPa for sound welds to 65.57 MPa for bonded welds at 2×10^6 cycles. At the macroscopic level there is no evidence of failure by shear. The fatigue fracture revealed cracks initiated from the root tip of kissing bond. © 2006 Springer Science + Business Media, Inc.

1. Introduction

Owing to their low density and good mechanical properties, aluminum alloys are increasingly employed in many important manufacturing areas, such as the automobile industry, aeronautics and the military [1]. However, traditional welding processes, when applied to several Al alloys, present a series of disadvantages such as porosity, cavities and hot cracking [2].

Friction stir welding (FSW) is a solid state joining method particularly well suited for aluminum alloys [3, 4], which are often difficult to be fusion welded without hot cracking, porosity or distortion. During welding, the material is frictionally heated to a temperature, at which it becomes more plastic. The heat of friction and plastic flow arising from the rotating tool produce significant microstructural changes, which lead to a local variation in the mechanical properties of the weld [5–9]. Details of the FSW process and the tool design are discussed in the literature [10, 11].

In engineering practice, most aluminum structures, such as ship hulls, ship superstructure, vehicle components, are welded and mainly subject to fatigue loading. The fatigue leads to damage of structural parts although the applied stress is quite low [12]. Fatigue behaviour is influenced by various factors that are the result of the weld shape. The main factors that influence the fatigue be-

haviour of welded structures are loading type, microstructure change and weld defects [13].

Recently, there has been growing interest in the kissing bond which is sometimes seen in the stir zone of etched cross-sectional FS weld, because it can include oxide particles. Okamura reported that a kissing bond remained as a vestige of the initial oxide layer in the cross-sectional stir zone for FSW parameters introducing low heat generation into the material, and concluded that the kissing bond in the stir zone did not affect mechanical properties of the weld [14]. Also Yutaka suggested that this kissing bond consists of a microstructure containing a high density of fine Al_2O_3 particles with an amorphous structure and did not affect the root-bend property of the weld [15]. However, the behaviour, especially the fatigue behaviour, of FS welds with a kissing bond still remains unclear. As fatigue is primary cause for 90% of all engineering failure [16], it is necessary to fully understand the fatigue property of FS welds with a kissing bond.

In this study, the fatigue properties of FS welds in 5083 aluminum alloy with a kissing bond (bonded welds) were investigated through the comparison with those of sound FS welds, and also the fracture surface of the FS welds was studied by scanning electron microscopy (SEM).

*Author to whom all correspondence should be addressed.

2. Experimental

The material used in this experiment was plates of rolled 5083-H321 aluminum alloy, and the chemical composition is (wt%) 4.3%Mg, 0.7%Mn, 0.25%Si, 0.12% Fe, 0.09%Cr, 0.09%Zn, Al bal.. The examined joined sheets had dimensions of 800 mm × 190 mm × 8 mm and were produced by China FSW Center Beijing FSW Technology Limited Company. Alloy 5083 is a weldable, strain hardening structural alloy suitable for marine applications, and 8 mm is the common thickness used in shipbuilding. The H321 designation represents a strain hardened and stabilized condition, with the alloy approximating the quarter-hard state after the thermal stabilisation treatment.

The cross-sections of the metallographic specimens were polished with alumina suspension, then etched by 2g NaOH + 100 ml H₂O solution about 15 min, then washed in distilled water 10 min and finally observed by the optical microscopy.

The fatigue tests were carried out in a high-frequency fatigue test machine with a capacity of 100 KN load. The fatigue specimens were machined perpendicular to the weld line. The weld was transverse to the stress axis in the S-N specimen (cross-weld). A sinusoidal load-time function was used, with the stress ratio R ($\sigma_{\min}/\sigma_{\max}$) set to 0.1. The oscillation frequency was in the interval of 85–90 Hz in laboratory air. To avoid the surface stress concentration, flash on the weld surface was removed and the edges of the specimens were rounded and polished. Shape and size of the fatigue test specimens are shown in Fig. 1. The fatigue data are expressed as stress range $\Delta\sigma$ (MPa) versus the corresponding life to failure N (i.e. number of cycles). Failed specimens were mounted and examined under an optical microscope as well as a PHILIPS XL-30 scanning electron microscopy (SEM).

Assessment of the fatigue behaviour of welds was obtained by applying statistical analysis to produce fatigue strength data as represented in SN-diagrams. The real area of interest to structures is the long life regime ($N > 10^6$ cycles), but pure aluminum and its alloys are regarded as not having a plateau in the stress-fatigue life relationship, unlike the other metal counterparts having b.c.c. and h.c.p. crystal structures [17]. Data were therefore calcu-

lated by a statistical evaluation to get the defined fatigue characteristic values at 2×10^6 cycles.

3. Results and discussion

3.1. Microstructure

Fig. 2 shows the macrographs of the transverse FS weld after etching. It can be seen that the welding flash is only released at the retreating side, where the direction of the tool rotation moves oppositely to the travel direction (anti-parallel). A striking feature of the macrostructure in Fig. 2 is the etched line in the stir zone which is identical to the position of the initial butt line. This line consists of a high density of fine Al₂O₃ particles with an amorphous structure [15]. Some papers [18–20] suggest that FSW is achieved by shear stress arising from rotation of the welding tool along the pin column surface. When shear stress works around the initial butt surfaces during FSW, it would break up the Al₂O₃ oxide layer on the surfaces and generate new oxide-free surfaces around the rotating pin. The broken products of the surface oxide may flow collectively during stirring, and form the wavy pattern in the stir zone. M. Peel suggested that low traverse rates or using a wider and coarser tool would eliminate the kissing bond [21]. However, fabricators may want to run FSW in a relatively high rate to obtain higher productivity, so it is not always possible to assume that they are free of a kissing bond. In another way, using a wider and coarser tool would make poor mechanical and metallographic properties of FS welds, and also the weld metal would be accumulated towards the stirrer shoulder that makes a bad effect on the welding process [22]. Hence the properties of welds with a kissing bond are needed to enhance confidence in the design and application of friction stir welded joints.

It should be noticed that the kissing bond is much different from the root flaws in FS welds. From Fig. 3, it can be seen that the kissing bond is just a faint line appearing in the stir zone (Fig. 3a) and the root flaw looks like a crack in the root part of the FS welds (Fig. 3b) [23]. The root flaw usually occurs if the pin length is too short for the plate thickness being welded, and this may also

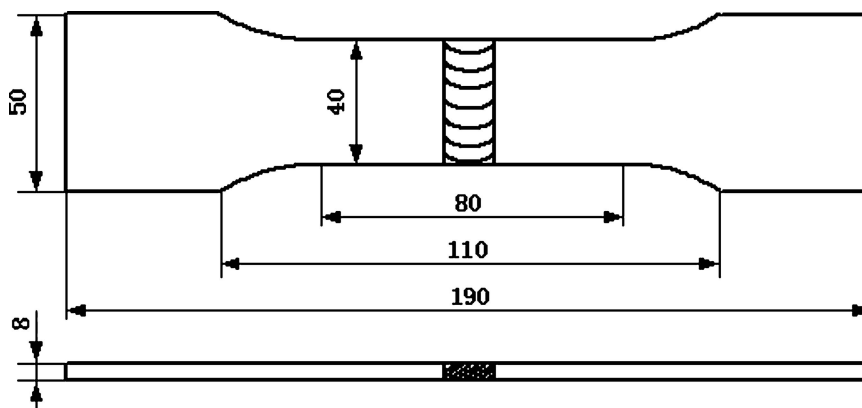


Figure 1 Shape and size of the fatigue test specimens (Unit: mm).

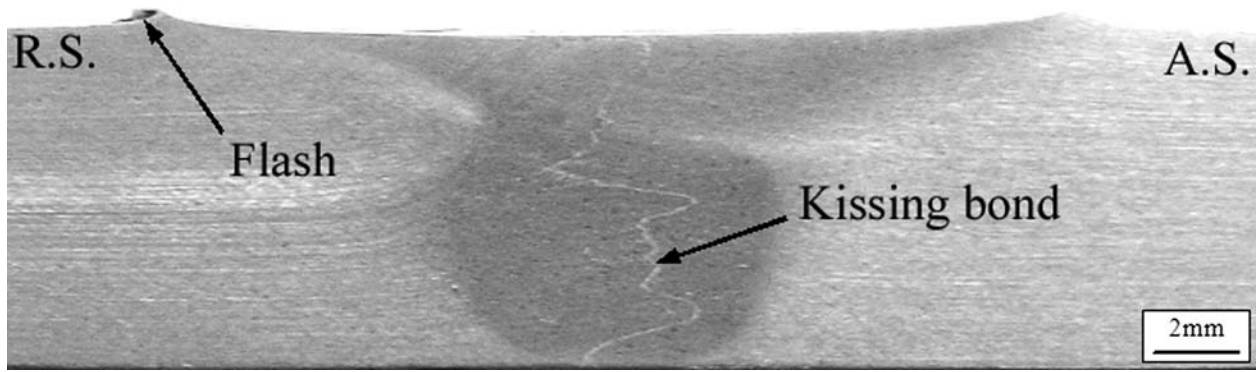


Figure 2 Transverse cross section of the FS welds.

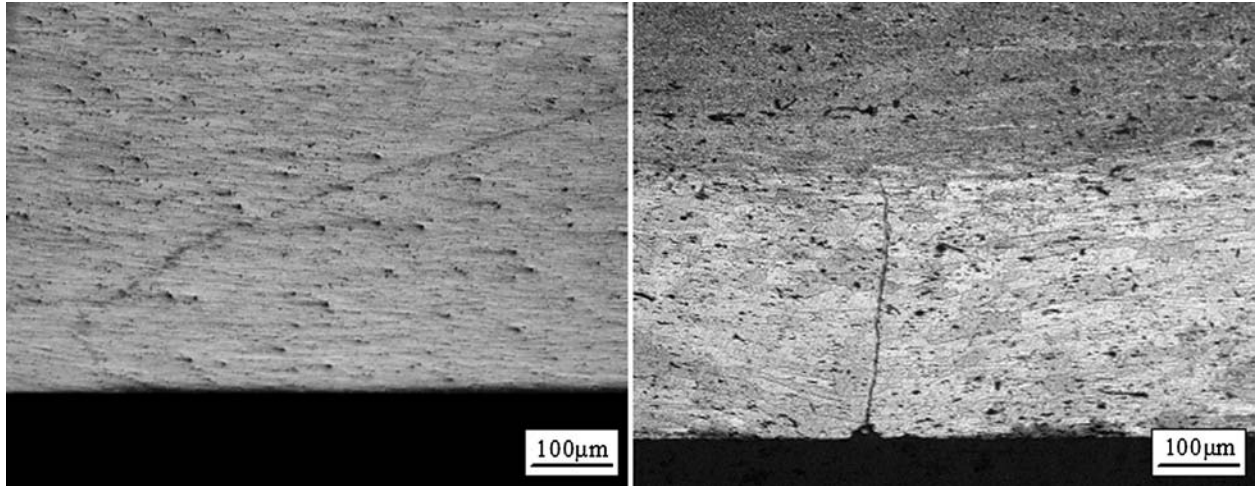


Figure 3 Optical micrograph of a kissing bond (a) and a root flaw (b).

occur due to low heat input or incorrect tool orientation. T. L. Dickerson reported that there was a partially bonding between the root flaw surfaces and the bonding increased with increasing distance from the weld root [24].

3.2. Fatigue property

As all the fractured specimens failed from the root tip of the kissing bond, the root region is the weakest site of FS welds with kissing bond, obviously. The degree of the kissing bond's influence on the fatigue property FS welds is determined by comparing the test results of bonded welds with the fatigue data of sound FS welds on 5083 alloys under the same stress ratio ($R = 0.1$) [25, 26].

Based on the loaded stress range and fatigue life, regression lines were drawn using least-squares fitting and the standard equation [27]:

$$S^m N = C \quad (1)$$

where S is the loaded stress range, N is the fatigue life, m and C are fitting constants. The regression lines fitted by Equation 1 represent the curve at the 50% of probability of survival (mean line) in Fig. 4.

For the test results of bonded welds, the regression line is expressed as:

$$\log N = 21.68 - 8.09 \log \Delta\sigma, \quad (2)$$

and for sound welds:

$$\log N = 20.08 - 6.61 \log \Delta\sigma \quad (3)$$

According to regression lines, comparison was made among the test results on the basis of the lives obtained at selected stress levels in Table I. It can be seen that the fatigue life of FS welds with a kissing bond is 21–43 times shorter than that of sound welds under the stress ratio $R = 0.1$. That means the root kissing bond can seriously shorten the fatigue life of the FS welds in both high stress/low-cycle and low stress/high-cycle regimes, especially in the former one.

In order to get the defined fatigue characteristic values at 2×10^6 cycles, a simplified statistical analysis was performed on the fatigue data at the 95% of probability with a lower 75% confidence limit. The main approximation adopted was to consider the standard deviation and the confidence interval constant.

TABLE I Comparison of the fatigue life

Weld	Stress range $\Delta\sigma_1$ /(MPa)	Fatigue life N_1	Stress range $\Delta\sigma_2$ /(MPa)	Fatigue life N_2
Bonded welds	153	1.0×10^4	95	4.7×10^5
Sound welds	153	4.3×10^5	95	1.0×10^7

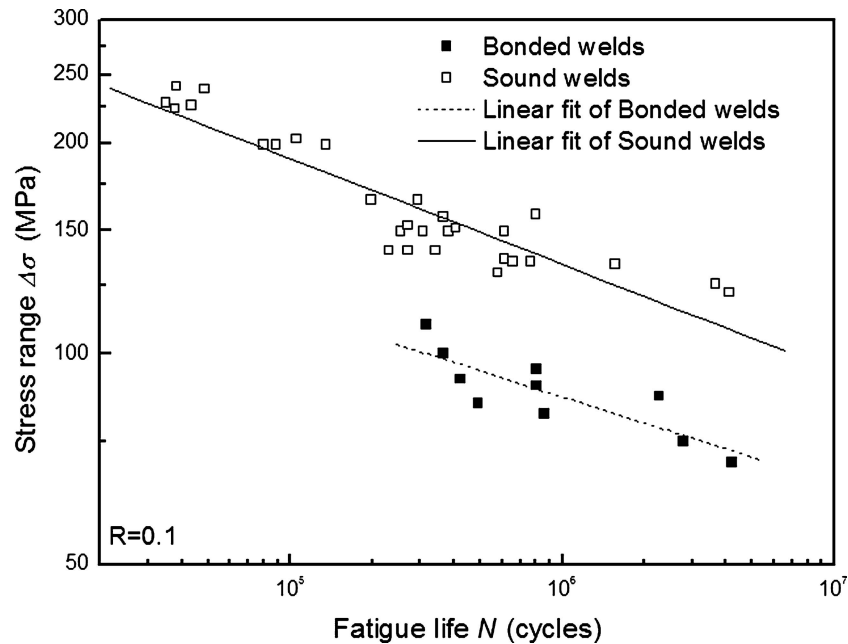


Figure 4 S-N curves of bonded and sound welds ($R = 0.1$).

The probability of the 95% means that 5 specimens failed out of 100 specimens tested at the same load; it is calculated as the difference between the average of the number of cycle and two times the standard error (s) (i.e. standard deviation or square root of the variance). Whereas, the 75% confidence limit estimation indicates that on 100 statements, which asserts that the results are given with a probability of 95%, 25 could be false.

According to the ‘Student’s t -Distribution’s Theory’ [28], used for the small-sample case, the fatigue characteristic values were calculated using the equation:

$$N_{0.95,0.75} = N_{0.95} - \frac{t_{0.75}\sqrt{2s}}{\sqrt{v}} \quad (4)$$

where $N_{0.95}$, estimated number of cycle, with a probability of the 95%; $N_{0.95, 0.75}$, estimated number of cycle, with the confidence of the 75%, of the data $N_{0.95}$, $t_{0.75}$ percentiles (considered at one tail), of the ‘Student’s t -distribution’, tabulated in the statistical literature; $\sqrt{2}$, is a correction factor, related to the error introduced in the estimation of the population variance; $v = (n - 2)$, are the degrees of freedom of the analysis; n is the number of specimens, 2 is the number of independent parameters estimated in the analysis.

The calculated results indicate that the fatigue characteristic values of each weld have decreased from 100.24 MPa for sound welds to 65.57 MPa for bonded welds at 2×10^6 cycles.

Currently, there are no standards relating specifically to the quality of friction stir welds, although some proprietary documents exist. In addition, welding quality standards also need to be related to design standards. Fig. 5 compares the test results of bonded welds and the data of flawed welds on 5083 alloy [24] with draft Eurocode 9 design curves [29] for transverse fusion butt welds. The spots with arrows may have a higher value for the weld, as they did not fail.

The design categories 14-3.2 and 18-3.2 relate respectively to partial-penetration and full-penetration welds made from one side. The design category 35-4 relates to double-sided (full-penetration) fusion welds. The first two categories pertain to cracking originating in the root and the highest category relates to weld toe cracking. As the present welds were made from one side and all the fractured specimens failed from weld root, it is the two lower detail categories that are of direct relevance. However, the higher category is shown for comparison purposes as single-sided friction stir welds may be required to replace arc welds made from both sides.

It can be seen from Fig. 5 that the data of bonded welds are remarkably higher than those of flawed welds. This can be explained by the partially bonding between the root flaw surfaces. And it is also can be seen that all the data of flawed welds fall above the two lower draft Eurocode category design lines, and only the data of bonded welds are beyond the category 35-4. Particularly, in the high-cycle region 10^6 cycles all the data obviously fall far away

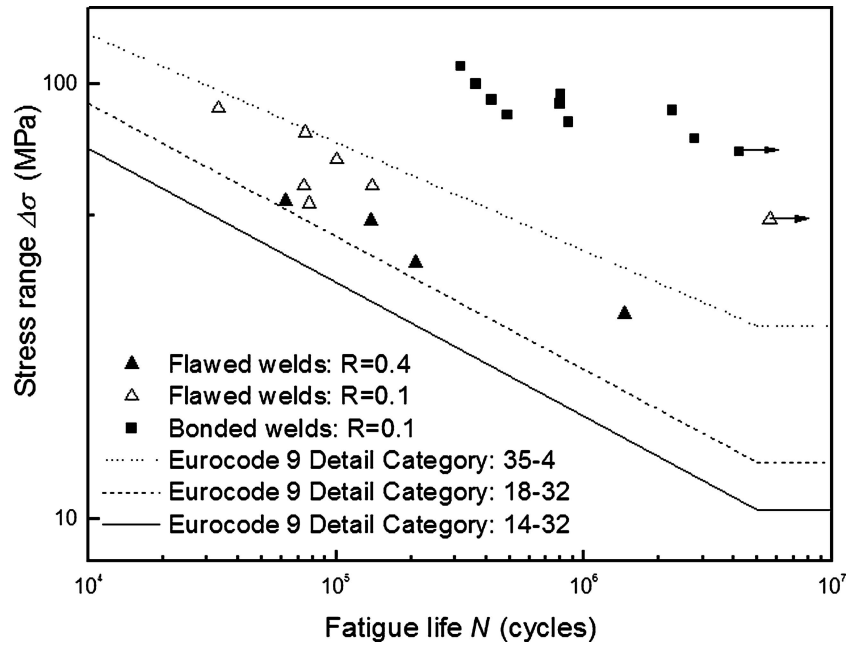


Figure 5 Comparison of fatigue data of flawed and bonded welds with Eurocode 9 design curves.

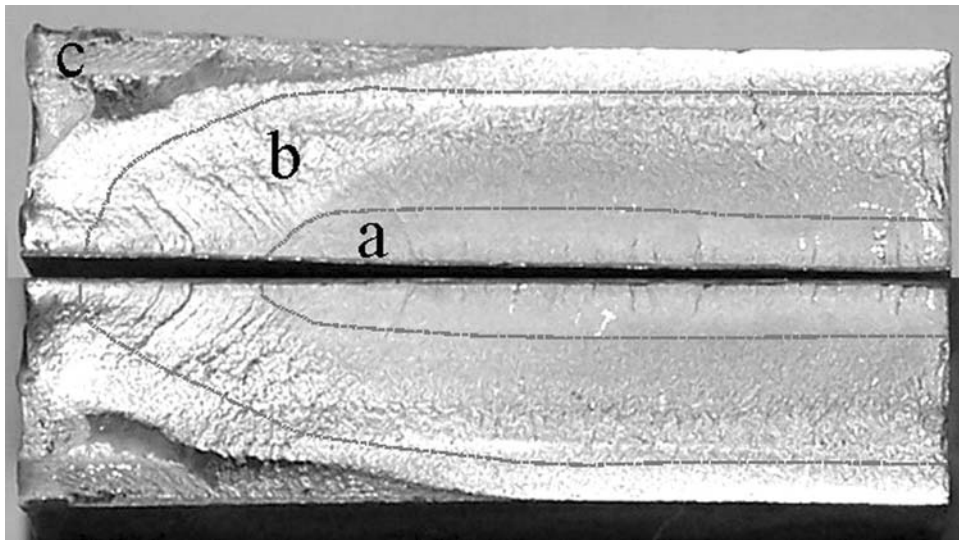


Figure 6 Macrograph of fracture surface (a) crack initiation; (b) stable crack growth; (c) final fracture.

above design categories 14-3.2. Hence, these comparison results indicate conservatism of the single-sided Eurocode 9 fusion weld design curves when applied to friction stir welds. It is therefore likely that the design line for friction stir butt welds can be raised to a higher level of stress compared to arc welds.

3.3. Fractography

At the macroscopic level there is no evidence of failure by shear for all the fractured specimens. Fig. 6 shows the fracture surface for the specimen tested at 95 MPa ($N = 8.02 \times 10^5$ cycles), which reveals regions of crack initiation, stable crack growth and final fracture. Fig. 7a illustrates that there are multiple crack initiations form-

ing at the root tip of kissing bond. The fine microscopic cracks, initially normal to the major stress axis, progressively grow and eventually coalesce to form one or more macroscopic cracks that also propagate through the microstructure in a direction normal to the major stress axis. The region of stable crack growth (Fig. 7b) exhibits relatively smooth areas containing distinct periodic markings, and also fine microscopic cracks and fatigue striations can be found in this region (Fig. 7c). A large population of shallow dimples varying size and shape (Fig. 7d) features reminiscent of locally ductile failure in the final fracture region.

The initiation of one or more microscopic cracks and their progressive growth through the alloy microstructure during repeated cyclic loading is attributed to be

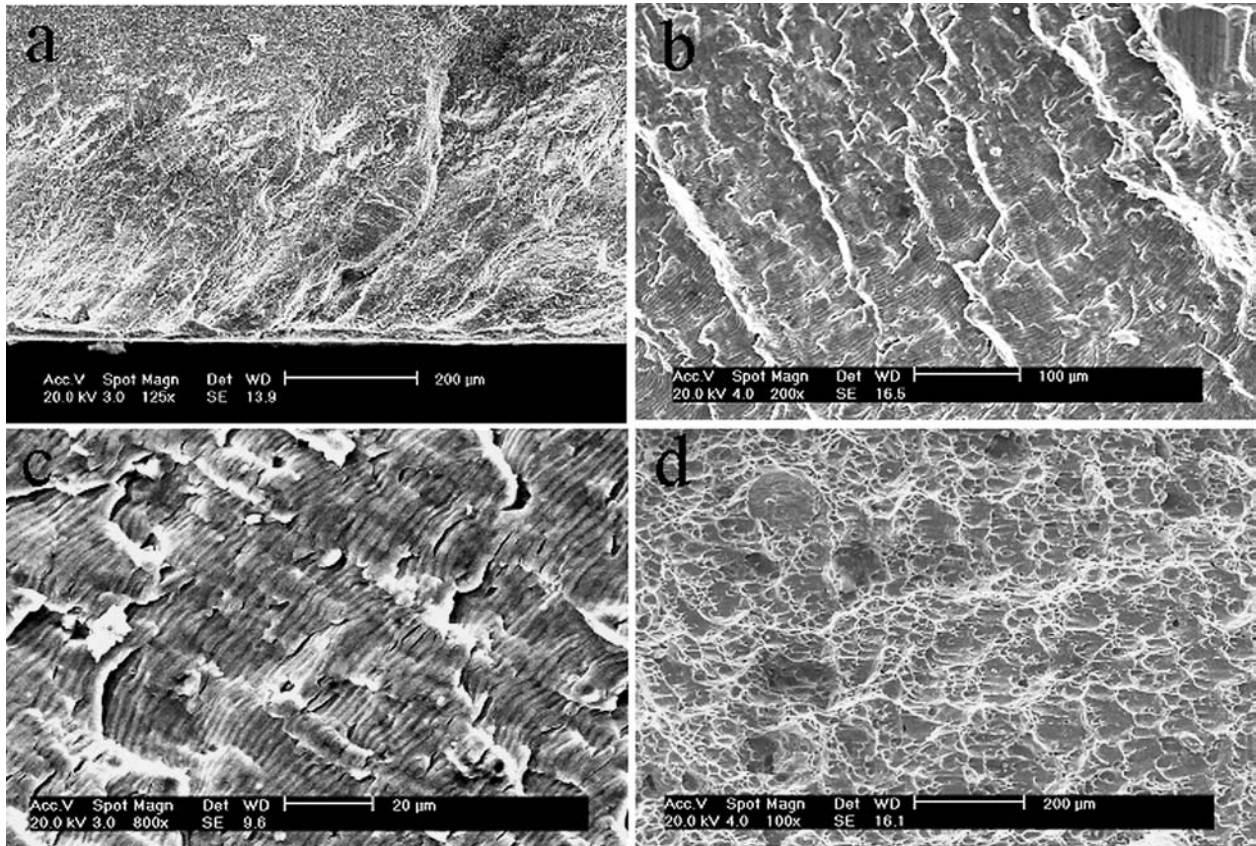


Figure 7 SEM images of fatigue fracture surfaces of the bonded weld.

the result of incremental accumulation of microplastic damage at the localized level. Yutaka reported that most of the Al_2O_3 particles are located on the grain boundaries in the faint line [15]. So under repeated cyclic loading, stress concentrations arise from a progressive build-up of dislocations at grain boundaries and at interfaces of the particles in the microstructure and finally the preferential plastic deformation results in a highly localized stress concentration at locations of grain boundary, with concomitant early nucleation of fine microscopic cracks.

It is clear that the kissing bond makes a reduction in crack initiation life under fatigue loading, and shortens the fatigue life of FS welds in a large degree. However, the test results are, at present, limited as experiments were carried out only with one thickness and with constant amplitude loading. Hence more and wider ranging tests are needed to be able to make a full understanding of the relationship between the kissing bond and fatigue properties of FS welds.

4. Conclusions

1. The fatigue life of bonded welds is 21–43 times shorter than that of sound welds under the stress ratio $R = 0.1$, and the fatigue characteristic values of each weld have decreased from 100.24 MPa for sound welds to 65.57 MPa for bonded welds at 2×10^6 cycles.

2. The fatigue fracture of FSW revealed regions of crack initiation, stable crack growth and overload, and cracks initiated from the root tip of kissing bond. The kissing bond makes a reduction in crack initiation life under fatigue loading, and shortens the fatigue life of FS welds in a large degree.

3. The design line for friction stir butt welds can be raised to a higher level of stress compared to arc welds. There are no universally accepted quality assurance procedures for friction stir welding, these need to be developed and incorporated into national and international standards.

Reference

1. S. J. MADDOX, *Int. J. Fatigue* **25** (2003) 1359.
2. A. HABOUDOU, P. PEYRE, A. B. VANNES and G. PEIX, *Mater. Sci. Eng. A* **363** (2003) 40.
3. Y. LI, L. E. MURR and E. A. TRILLO, *J. Mater. Sci.* **19** (2000) 1047.
4. M. A. SUTTON, B. Y. YANG, A. P. REYNOLDS and R. TAYLOR, *Mater. Sci. Eng. A* **323** (2002) 160.
5. C. G. RODES, M. W. MAHONEY, W. H. BINGEL, R. A. SPURLING and C. C. BAMPTON, *Scripta Mater.* **36** (1997) 69.
6. O. V. FLORES, C. KENNEDY and L. E. MURR, *Scripta Mater.* **38** (1998) 703.
7. M. W. MAHONEY, C. G. RODES, J. G. FLINTOFF, R. A. SPURLING and W. H. BINGEL, *Metall. Mater. Trans. A* **29** (1998) 1955.
8. S. BENAVIDES, Y. LI, L. E. MURR, D. BROWN and J. C. MCCLURE, *Scripta Mater.* **41** (1999) 809.
9. K. V. JATA and S. L. SEMIATIN, *ibid.* **43** (2000) 743.

10. C. J. DAWES and W. M. THOMAS, *Weld J.* **75** (1996) 41.
11. G. CAMPBELL and T. STOTLER, *Weld J.* **78** (1999) 45.
12. H. J. ROGERSON, *Weld. Res. Abroad* **10** (1969) 60.
13. J. E. TOMLINSON and J. L. WOOD, *Brit. Weld. Journal* **GB7** (1960) 22.
14. H. OKAMURA, K. AOTA, M. SAKAMOTO, M. EZUMI and K. IKEUCHI, *J. Jpn. Weld Soc.* **19** (2001) 446.
15. Y. S. SATO, F. YAMASHITA and Y. SUGIURA, *Scripta Mater.* **50** (2004) 365.
16. L. HOU, in "Fracture Behavior and Assessment of Welded Structure" (China Machine Press, Beijing, 2000) p. 221.
17. T. S. SRIVATSAN, *Mater. Design* **23** (2002) 141.
18. D. P. FIELD, T. W. NELSON, Y. HOVANSKI and K. V. JATA, *Metall Mater. Trans. A* **32** (2001) 2869.
19. Y. S. SATO, H. KOKAWA, K. IKEDA, M. ENOMOTO, S. JOGAN and T. HASHIMOTO, *Metall Mater. Trans. A* **32** (2001) 941.
20. S. H. C. PARK, Y. S. SATO, H. KOKAWA, *Metall Mater. Trans. A* **34** (2003) 987.
21. M. PEEL, A. STEUWER, M. PREUSS and P. J. WITHERS, *Acta Mater.* **51** (2003) 4791.
22. M. BOZ and A. KURT, *Mater. Design* **25** (2004) 343.
23. C. ZHOU, X. YANG and G. LUAN, *Rare Metal. Mat. Eng.* (in press).
24. T. L. DICKERSON and J. PRZYDATEK, *Int. J. Fatigue* **25** (2003) 1359.
25. C. DAWES and W. THOMAS, *TWI Bull* **6** (1995) 493.
26. S. LOMOLINO, R. TOVOB and J. DOS SANTOS, *Int. J. Fatigue* **27** (2005) 305.
27. T. R. GURUEY, in "Fatigue of Welded Structures" (Cambridge University Press, London, 1979) p. 214.
28. C. CHATFIELD, *Statistic for technology*, in "A course in applied statistics" (Chapman & Hall, London, 1978) p. 105.
29. Eurocode 9. Design of aluminum structures: part 2: structures susceptible to fatigue. Brussels: CEN, 1998 ENV, 1999–2002.

*Received 4 June
and accepted 28 September 2005*